Co-Processing of Jatropha-Derived Bio-Oil with Petroleum Distillates over Mesoporous CoMo and NiMo Sulfide Catalysts

Shih-Yuan Chen [1],* , Masayasu Nishi [1], Takehisa Mochizuki [1], Hideyuki Takagi [1], Akira Takatsuki [1], Wuttichai Roschat [2,3], Makoto Toba [1] and Yuji Yoshimura [4]

[1] Research Institute of Energy Frontier (RIEF), Department of Energy and Environment, National Institute of Advanced Industrial Science and Technology (AIST), 16-1 Onogawa, Tsukuba, Ibaraki 305-8569, Japan; m.nishi@aist.go.jp (M.N.); t.mochizuki@aist.go.jp (T.M.); hide-takagi@aist.go.jp (H.T.); akira-takatsuki@aist.go.jp (A.T.); m.toba@aist.go.jp (M.T.)

[2] Program of Chemistry, Faculty of Science and Technology, Sakon Nakhon Rajabhat University, 680 Nittayo Rd., Mueang District, Sakon Nakhon 47000, Thailand; roschat1@gmail.com

[3] Center of Excellence on Alternative Energy, Research and Development Institute, Sakon Nakhon Rajabhat University, 680 Nittayo Rd., Mueang District, Sakon Nakhon 47000, Thailand

[4] Materials for Energy Research Unit, National Metal and Materials Technology Center (MTEC), Pahonyothin Rd. Klong 1, Klong Luang Pathumtani 12120, Thailand; y.yoshimura@aist.go.jp

* Correspondence: sy-chen@aist.go.jp; Tel.: +81-29-861-2680; Fax: +81-29-861-4532

Abstract: The co-processing of an unconventional type of Jatropha bio-oil with petroleum distillates over mesoporous alumina-supported CoMo and NiMo sulfide catalysts (denoted CoMo/γ-Al$_2$O$_3$ and NiMo/γ-Al$_2$O$_3$) was studied. Either a stainless-steel high-pressure batch-type reactor or an up-flow fixed-bed reaction system was used under severe reaction conditions (330–350 °C and 5–7 MPa), similar to the conditions of the conventional diesel hydrodesulfurization (HDS) process. To understand the catalytic performance of the mesoporous sulfide catalysts for co-processing, we prepared two series of oil feedstocks. First, model diesel oils, consisting of hydrocarbons and model molecules with various heteroatoms (sulfur, oxygen, and nitrogen) were used for the study of the reaction mechanisms. Secondly, low-grade oil feedstocks, which were prepared by dissolving of an unconventional type of Jatropha bio-oil (ca. 10 wt %) in the petroleum distillates, were used to study the practical application of the catalysts. Surface characterization by gas sorption, spectroscopy, and electron microscopy indicated that the CoMo/γ-Al$_2$O$_3$ sulfide catalyst, which has a larger number of acidic sites and coordinatively unsaturated sites (CUS) on the mesoporous alumina framework, was associated with small Co-incorporated MoS$_2$-like slabs with high stacking numbers and many active sites at the edges and corners. In contrast, the NiMo/γ-Al$_2$O$_3$ sulfide catalyst, which had a lower number of acidic sites and CUS on mesoporous alumina framework, was associated with large Ni-incorporated MoS$_2$-like slabs with smaller stacking numbers, yielding more active sites at the brims and corresponding to high hydrogenation (HYD) activity. Concerning the catalytic performance, the mesoporous CoMo/γ-Al$_2$O$_3$ sulfide catalyst with large CUS number was highly active for the conventional diesel HDS process; unfortunately, it was deactivated when oxygen- and nitrogen-containing model molecules or Jatropha bio-oil were present in the oil feedstock. In contrast, the mesoporous NiMo/γ-Al$_2$O$_3$ sulfide catalyst, which had a high HYD activity and low affinity for heteroatoms, was efficient in the simultaneous removal of those heteroatoms from model diesel oils, and, in particular, Jatropha bio-oil co-fed with petroleum distillates. This could allow the production of a drop-in diesel-like fuel, which would be a greener fuel and reduce the CO$_2$ emissions and hazardous exhaust gases produced by the transport sector, reducing the burden on the environment.

Keywords: mesoporous sulfide catalyst; co-processing; hydrotreating; bio-oil; resistances to oxygen and nitrogen; diesel-like green fuel

1. Introduction

In accord with the Paris Agreement on global climate action [1], the Royal Thai Government has legislated "The Alternative Energy Development Plan 2015–2036 (AEDP2015-2036)" to reduce the nation's dependence on fossil energy and to suppress fossil energy-related CO_2 emissions by the use of sustainable resources, such as waste- and biomass-derived energy and fuels [2]. According to the AEDP2015-2036 project, the utilization of waste plastic-derived pyrolysis oil and biomass-derived fuels (known as biofuels) in the transport sector is to be increased from the current value of 6.3% to 25% by 2036. Among the biofuels, bioethanol, biodiesel, and biomethane have been successfully synthesized at an industrial scale [3–5]. However, the technology for the production and utilization of alternative biofuels, i.e., bio-oil and hydrogenated vegetable oil (HVO), is still in the early stages of research and development [6–8]. Bio-oil is conventionally produced by the decomposition of woody biomass waste, such as pine or cedar, through the fast pyrolysis technique with or without the aid of solid catalysts [9]. The pine- or cedar-derived bio-oils with large amounts of oxygen-containing compounds, such as phenol derivatives, can be further upgraded to a gasoline-like fuel through hydrodeoxygenation (HDO) over transition metal catalysts and mesoporous sulfide catalysts under severe reaction conditions [6,10,11]. On the other hand, the transformation of vegetable oils to HVO as a drop-in diesel-like fuel can also be carried out using HDO technology [12,13]. However, recent studies have indicated that transition metal catalysts and mesoporous sulfide catalysts are seriously deactivated by the large numbers of oxygen-containing compounds present in bio-oil or vegetable oils under the severe HDO conditions [10,12]. Several processing steps, such as in situ regeneration to protect the catalytically active sites, are required to reduce catalyst deactivation.

We had previously succeeded in carrying out the fast pyrolysis of Jatropha biomass waste (non-edible biomass comprising cellulose, hemicellulose, lignin, and residual Jatropha oil) into an unconventional type of bio-oil in a pilot plant. The plant, which is in Thailand, has a relatively large production capacity of ca. 20 kg h^{-1} [14–16]. This Jatropha bio-oil naturally consists of fatty acids, fatty acid methyl esters, and amides (>50 wt %) in addition to relatively small amounts of hydrocarbons, and oxygen- and nitrogen-containing heterocyclic compounds. It is a mixture of partially hydrogenated vegetable oil and bio-oil, which is unlike conventional cedar- or pine-derived bio-oils. Our earlier studies showed that Jatropha bio-oil contains large amounts of heteroatoms (oxygen > 20 wt %, nitrogen > 3 wt %, and sulfur > 500 ppm) [9,14–16], which may severely affect the catalytic performance of the transition metal catalysts and mesoporous sulfide catalysts frequently used in the upgrading process. However, mesoporous sulfide catalysts possess high activities and robust structures in the co-processing of heteroatom-containing bio-oil with petroleum distillates to produce clean fuels compared to transition metal catalysts. In this paper, the catalytic performance of mesoporous sulfide catalysts in the co-processing of model diesel oils or the Jatropha bio-oil mixed with petroleum distillates is reported for the first time. This co-processing is similar to the conventional diesel hydrodesulfurization (HDS) process. There are two reasons for the co-processing of Jatropha bio-oil with light gas oil (LGO), the diesel fraction of raw petroleum distillate. First, the carbon chain length distribution of Jatropha bio-oil is near that of petrodiesel fuel. Secondly, the hydrotreated oil that is produced from the hydrotreating of pure Jatropha bio-oil over mesoporous sulfide catalysts still contains large numbers of heteroatom species. In fact, the catalytically active sites are deactivated by the poisons of oxygen- and nitrogen-containing compounds in Jatropha bio-oil. The deactivation of mesoporous sulfide catalysts by oxygen- and nitrogen-containing compounds could be retarded by the presence of sulfur-containing compounds that are naturally present in LGO (i.e., the sulfidation of deactivated catalysts). Moreover, the composition and fuel properties of hydrotreated oils would be similar to those of petrol-diesel fuel obtained by the conventional diesel HDS process. In this study, we paid special attention to the influences of oxygen- and nitrogen-containing compounds on the

catalytically active sites of mesoporous sulfide catalysts during co-processing. The possible routes for the co-processing of Jatropha bio-oil co-fed with LGO over mesoporous sulfide catalysts into a drop-in diesel-like fuel with a low heteroatom content as a greener transport fuel with low environmental impact are further discussed.

2. Results and Discussion

2.1. Characterizations of the Mesoporous Sulfide Catalysts

The wide-angle X-ray diffraction (XRD) patterns show that the crystallinity of the mesoporous $CoMo/\gamma$-Al_2O_3 sulfide catalyst is slightly lower than that of the mesoporous $NiMo/\gamma$-Al_2O_3 sulfide catalyst (Figure 1A). The corresponding N_2 adsorption-desorption isotherms show that both catalysts possess a classical type-IV isotherm with an H_1 hysteresis loop in the relatively high P/P_0 region (Figure 1B), suggesting the presence of a largely mesoporous framework. Table 1 tabulates the physicochemical property of the mesoporous $CoMo/\gamma$-Al_2O_3 and $NiMo/\gamma$-Al_2O_3 sulfide catalysts. The N_2 physisorption data reveal that the specific surface area (S_{BET}), total pore volume (V_{total}), and pore size (Φ_p) of the mesoporous $CoMo/\gamma$-Al_2O_3 and $NiMo/\gamma$-Al_2O_3 sulfide catalysts are independent of Ni and Co. (denoted as the promoters), whereas the NH_3 and NO uptakes vary slightly. The differential heat of NH_3 adsorption study further indicates that the acidic strength and capacity of mesoporous sulfide catalysts can be enhanced if Ni is replaced by Co (Figure 2). This result implies that the surface fine structures of the mesoporous $CoMo/\gamma$-Al_2O_3 and $NiMo/\gamma$-Al_2O_3 sulfide catalysts are slightly different from each other, such as the acidic sites, coordinatively unsaturated sites (CUS), and brim sites. A previous study has shown that the activity and selectivity of mesoporous sulfide catalysts in the hydrotreating of crude oils are highly related to their surface fine structures, which, in turn, influences the composition and fuel properties of the hydrotreated oils [17].
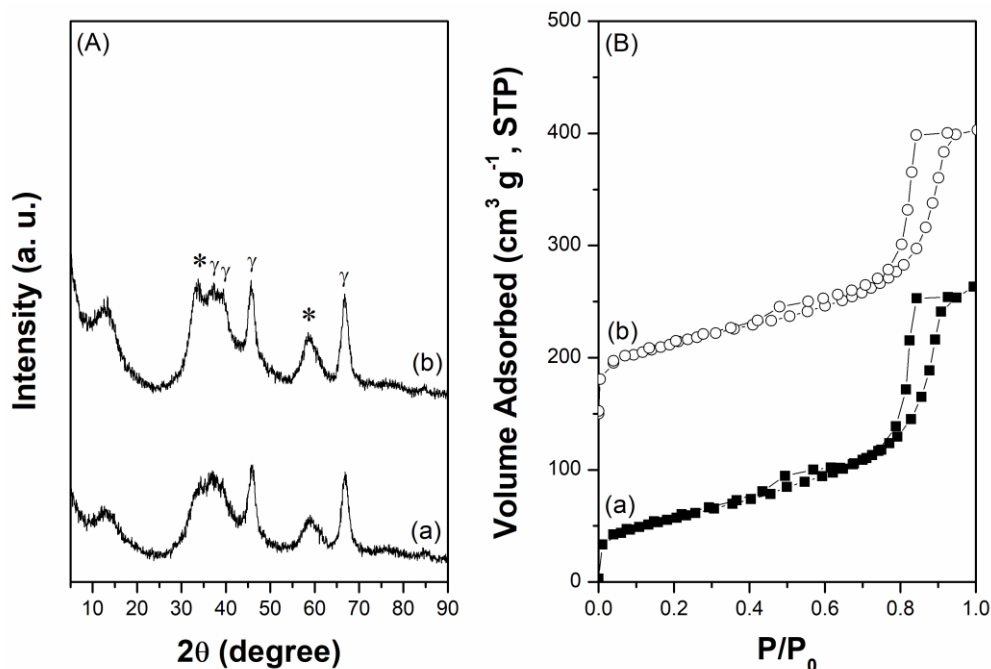

Figure 1. (**A**) Wide-angle XRD patterns and (**B**) N_2 adsorption-desorption isotherms of mesoporous sulfide catalysts (a) $CoMo/\gamma$-Al_2O_3 and (b) $NiMo/\gamma$-Al_2O_3. The asterisk and gamma (γ) represent the MoS_2-like slabs and γ-Al_2O_3 phase, respectively.

Table 1. Physicochemical properties of mesoporous sulfide catalysts.

Sulfided Catalysts	S_{BET} ($m^2\ g^{-1}$)	V_{total} ($cm^3\ g^{-1}$)	Φ_P (nm)	MoS$_2$-Like Slabs [a]			NH$_3$ Uptake ($mmol\ g^{-1}$)	NO Uptake ($mmol\ g^{-1}$)
				Stacking Number	Length (nm)	Height (nm)		
CoMo/γ-Al$_2$O$_3$	205	0.38	12	3.8 ± 0.86	4.5 ± 1.2	2.0 ± 0.53	0.92	0.11
NiMo/γ-Al$_2$O$_3$	204	0.41	12	2.6 ± 0.71	5.9 ± 1.4	1.5 ± 0.56	0.77	0.093

[a] The average data obtained from the HRTEM images.
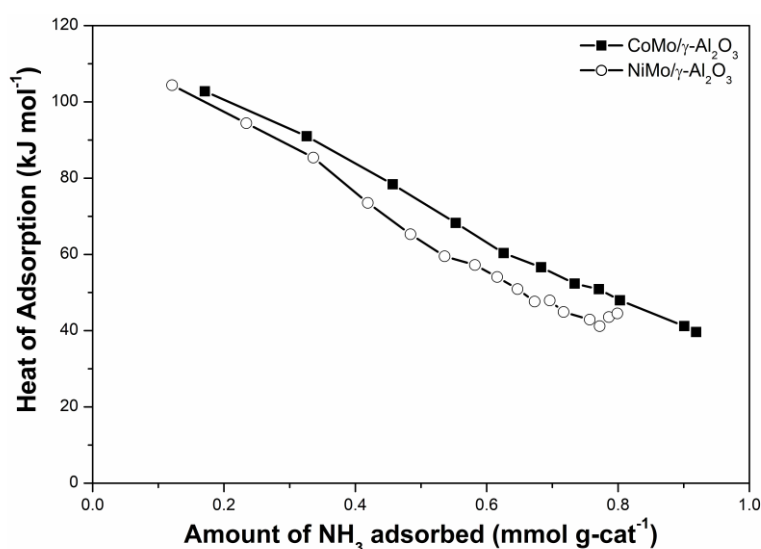
Figure 2. Differential heat of NH$_3$ adsorption over mesoporous sulfide catalysts.

To understand the surface fine structures better, mesoporous sulfide catalysts were investigated by in situ diffuse reflectance infrared Fourier transform (DRIFT) spectroscopy using pyridine and NO as probe molecules. High-resolution transmission electron microscopy (HRTEM) images were also obtained. In the in situ DRIFT spectra with pyridine adsorption (Figure 3A), the characteristic DRIFT signals centered at 1442 and 1540 cm^{-1} are assigned to pyridine adsorbed on Lewis and Bronsted acid sites, respectively [18–20]. The DRIFT signal centered at 1442 cm^{-1} is stronger than others, indicating that mesoporous sulfide catalysts are mostly related to Lewis solid acids. For the in situ DRIFT spectra with NO adsorption (Figure 3B), the characteristic DRIFT signals centered at 1665 and around 1832–1847 cm^{-1} are assigned to NO adsorbed on the CUS regions nearby the MoS$_x$ and CoS$_x$ (or NiS$_x$) species, respectively [21]. It is worth noting that NO preferentially adsorbs on the CUS regions at the edges or corners of the Co- and Ni-incorporated MoS$_2$-like slabs but it does not adsorb on the molybdenum(VI) cations or the mesoporous alumina framework [22]. The surface fine structures of the mesoporous sulfide catalysts were directly observed by the HRTEM technique (Figure 4). The HRTEM images show that the mesoporous sulfide catalysts contain well-dispersed MoS$_2$-like slabs in which the stacking number, length, and height are varied slightly with the incorporation of Co. and Ni. The average values of Co- or Ni-incorporated MoS$_2$-like slabs obtained by statistical methods are tabulated in Table 1. The Co-incorporated MoS$_2$-like slabs (stacking number ≈ 3.8, width ≈ 4.5 nm, height ≈ 2.0 nm) are obviously smaller but higher than the Ni-incorporated counterparts (stacking number ≈ 2.6, width ≈ 5.9 nm, height ≈ 1.5 nm).
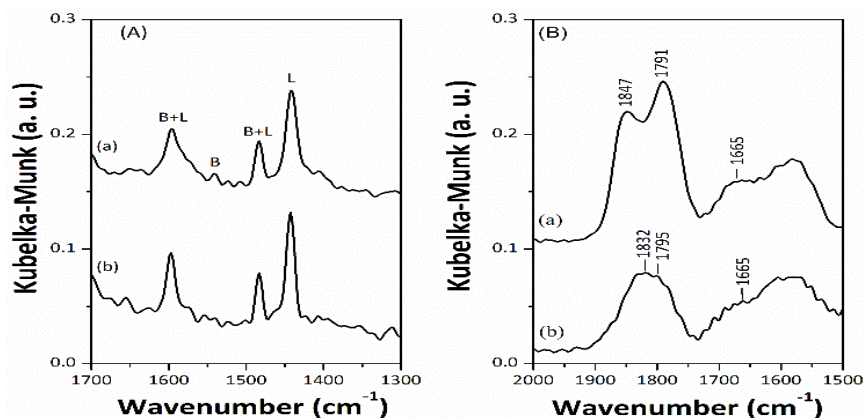
Figure 3. In situ diffuse reflectance infrared Fourier transform (DRIFT) spectra of (**A**) pyridine and (**B**) NO adsorbed on mesoporous sulfide catalysts (a) CoMo/γ-Al$_2$O$_3$ and (b) NiMo/γ-Al$_2$O$_3$. The B and L represent the Brønsted and Lewis sites, respectively.
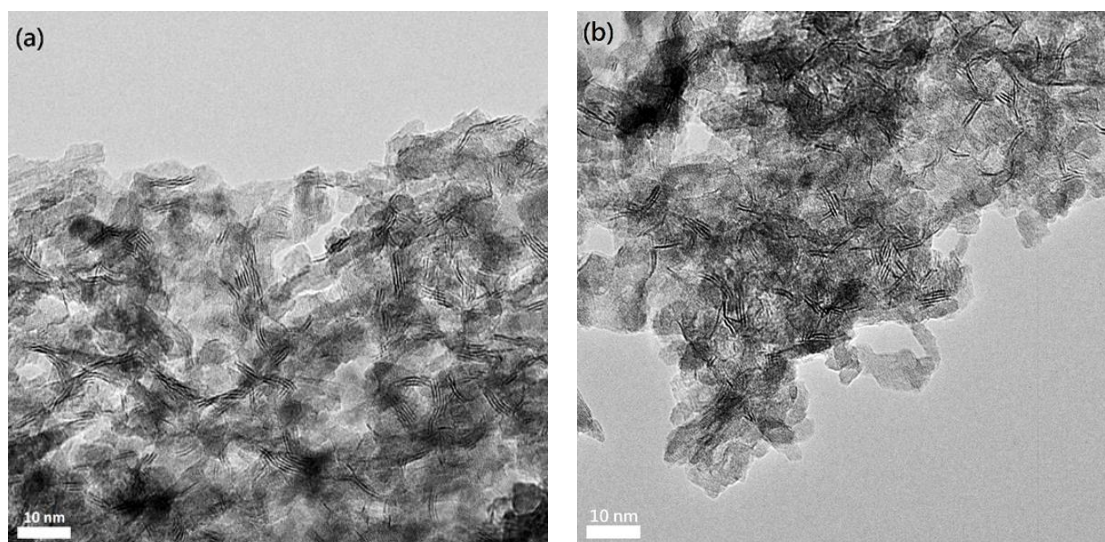

Figure 4. High-resolution transmission electron microscopy (HRTEM) images of mesoporous sulfide catalysts (**a**) CoMo/γ-Al$_2$O$_3$ and (**b**) NiMo/γ-Al$_2$O$_3$.

The chemical environments of the mesoporous CoMo/γ-Al$_2$O$_3$ and NiMo/γ-Al$_2$O$_3$ sulfide catalysts prepared by similar procedures have been previously examined by extended X-ray absorption fine structure (EXAFS) measurements [22–24]. The unsupported MoS$_2$ crystal was used as a reference material, where the coordination numbers of molybdenum and sulfur (denoted N(Mo) and N(S), respectively) were close to 6. The EXAFS calculations revealed that mesoporous sulfide catalysts possessed very small N(Mo) values of ca. 2–3 and moderate N(S) values of ca. 4.5–5.5, indicating the presence of highly-dispersed MoS$_2$-like slabs. Moreover, the mesoporous CoMo/γ-Al$_2$O$_3$ sulfide catalyst with smaller N(Mo) and N(S) values should have smaller MoS$_2$-like slabs. This speculation is supported by our characterization results. Combining the wide-angle XRD, gas adsorption, in situ DRIFT, and HRTEM studies with previous EXAFS data, the differences in surface fine structures between the mesoporous CoMo/γ-Al$_2$O$_3$ and NiMo/γ-Al$_2$O$_3$ sulfide catalysts are proposed in Scheme 1. The mesoporous CoMo/γ-Al$_2$O$_3$ sulfide catalyst has a relatively large number of acidic sites and CUS, which is presumably due to the presence of the small Co-incorporated MoS$_2$-like slabs with high stacking numbers on the mesoporous alumina framework. These small Co-incorporated MoS$_2$-like slabs should have more active sites at the edges or corners. On the other hand, the mesoporous

NiMo/γ-Al$_2$O$_3$ sulfide catalyst has a relatively small number of acidic sites and CUS, probably related to the large Ni-incorporated MoS$_2$-like slabs with lower stacking numbers impregnated on the mesoporous alumina framework. These large Ni-incorporated MoS$_2$-like slabs may contribute to the larger number of active sites at the brims.
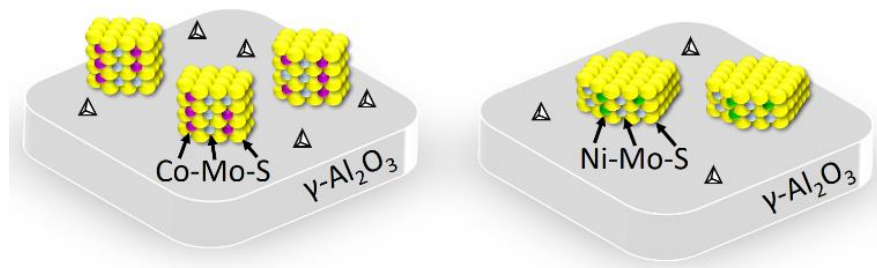
Scheme 1. Proposed surface fine structures of the mesoporous CoMo/γ-Al$_2$O$_3$ and NiMo/γ-Al$_2$O$_3$ sulfide catalysts, where pink and green spheres represent the Co. and Ni species in MoS$_2$-like slabs, respectively.

2.2. Hydrotreating Model Diesel Oils

The ability of the mesoporous CoMo/γ-Al$_2$O$_3$ and NiMo/γ-Al$_2$O$_3$ sulfide catalysts to simultaneously remove heteroatoms (sulfur, oxygen, and nitrogen) from model diesel oils A–D (Table S1) was examined using a high-pressure stainless-steel batch-type reactor at 330 °C and 5 MPa of H$_2$ for 1 h (Figure 5). When model diesel oil A was used as an oil feedstock, the sulfur contents of hydrotreated oils over mesoporous sulfide catalysts were remarkably reduced to 74–107 ppm. Apparently, the mesoporous CoMo/γ-Al$_2$O$_3$ sulfide catalyst is superior to mesoporous NiMo/γ-Al$_2$O$_3$ sulfide catalyst in the removal of sulfur from model diesel oil A. It is reasonable to surmise that the Co-incorporated MoS$_2$-like slabs result in higher activity in the HDS of dibenzothiophene (DBT) and 4,6-dimethyldibenzothiophene (DMDBT) than the Ni-incorporated counterparts. When model diesel oils B–D containing stearic acid or quinoline were used as oil feedstocks, the sulfur- and nitrogen-containing compounds mostly remained in the hydrotreated oils treated over the mesoporous sulfide catalysts, whereas the oxygen-containing compounds were mostly removed (>98%). With mesoporous sulfide catalysts, it is easier to achieve the HDO of stearic acid than the HDS of DBT and DMDBT and the hydrodenitrogenation (HDN) of quinoline. In addition, the heteroatom concentrations of the hydrotreated oils over the mesoporous NiMo/γ-Al$_2$O$_3$ sulfide catalyst are obviously lower than those over the mesoporous CoMo/γ-Al$_2$O$_3$ sulfide catalyst. The influences of oxygen- and nitrogen-containing compounds on the hydrotreating performance of mesoporous sulfide catalysts in the hydrotreating of model diesel oils B–D may be related to the interactions of model compounds adsorbed on the catalytically active sites and other surface fine structures.

To understand the catalytic behavior of the mesoporous sulfide catalysts in the hydrotreating of model diesel oils A–D, the possible reaction pathways for HDS, HYD, HDO, and HDN are illustrated in Scheme 2 [25–27]. In the HDS of DBT, biphenyl is formed by the direct desulfurization (DDS) pathway, whereas cyclohexylbenzene and cyclopentylmethylbenzene are formed by the HYD and subsequent isomerization/desulfurization pathway. Bicyclohexyl and cyclopentylmethyl cyclohexane are obtained if the DDS and HYD products are further hydrogenated. Similarly, the HDS of DMDBT can be catalyzed by the DDS and HYD pathways. In the HDO of stearic acid, heptadecane is formed by the decarboxylation/decarbonylation (DeCO$_x$) pathway, whereas octadecane is formed by the HYD and subsequent deoxygenation pathways. In the HDN of quinoline, propylbenzene is formed by the direct denitrogenation (DDN) pathway, whereas propylcyclohexane is formed by HYD and subsequent denitrogenation pathway. In the HYD of tetralin, *cis*- and *trans*-decalin are formed by the isomerization and HYD of octalin as hydrogenated intermediates. Based on the proposed reaction mechanisms, the catalytic behavior of the mesoporous sulfide catalysts in these model reactions can be

thoroughly discussed, including the hydrotreating activity, the conversion of model compounds, and the selectivity for products (Figures 6 and 7). The detailed data are tabulated in Tables S2–S3 (ESI). The hydrotreating activity was calculated by dividing the molar faction of oil desulfurized by the catalyst after the first hour of reaction. Figure 6 shows that the decreases in hydrotreating activity and conversions of DBT, DMDBT, and tetralin follow the order: model diesel oils A > B >> C > D. The HDS of DMDBT and the HYD of tetralin over the mesoporous sulfide catalysts are particularly inhibited by quinoline in model diesel oils C and D. However, stearic acid and quinoline were almost consumed in a short reaction period although they seem to compete with each other for the catalytically active sites. These observations suggest, again, that the catalytically active sites for the HDS of DBT and DMDBT, the HDO of stearic acid, the HDN of quinoline, and the HYD of tetralin over the mesoporous sulfide catalysts are the same or are close to each other. As estimated from the catalytic data, the competition among these reactions follows the order: HDN of quinoline $\approx$ HDO of stearic acid > HDS of DBT >> HDS of DMDBT $\approx$ HYD of tetralin, which should be directly related to the sequence of competitive adsorption of various model compounds on the catalytically active sites. Therefore, it can be said that the catalytically active sites of mesoporous sulfide catalysts give high priority to the HDN of quinoline and the HDO of stearic acid; thus, the HDS of DBT and DMDBT, and the HYD of tetralin are strongly inhibited at the same time, particularly for the latter two model compounds.
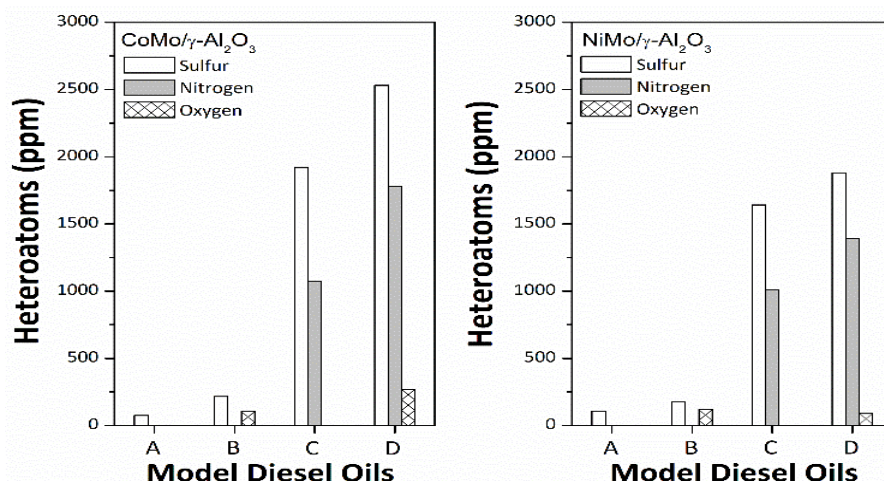

Figure 5. The activity of mesoporous sulfide catalysts to simultaneously remove heteroatoms from the model diesel oils A–D at 330 °C and 1 h under a pressurized atmosphere of H_2 (5 MPa), where the model diesel oils were made by 70% of n-hexadecane and 30% of tetralin with addition of sulfur-, oxygen- and nitrogen-containing model molecules (please see Table S1, ESI).
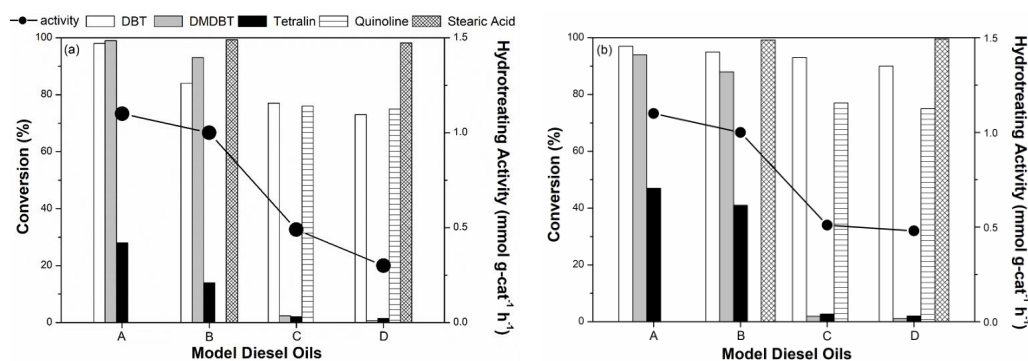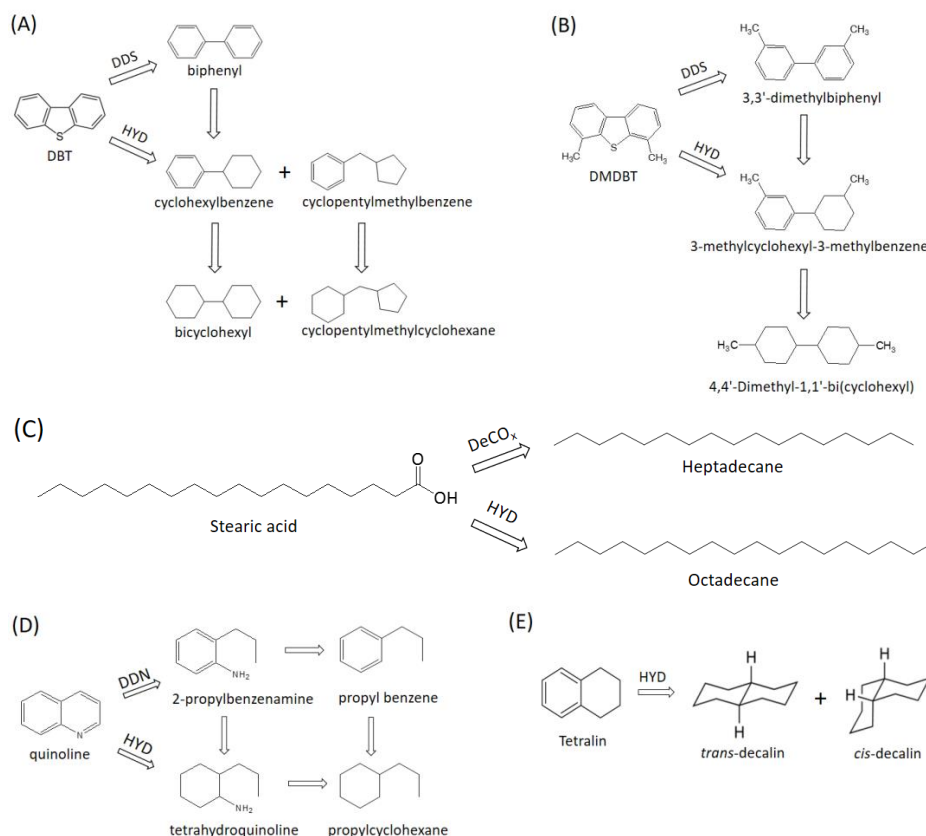

Figure 6. The catalytic activities of the mesoporous sulfide catalysts (**a**) CoMo/γ-Al$_2$O$_3$ and (**b**) NiMo/γ-Al$_2$O$_3$ in the hydrotreating of model diesel oils A–D at 330 °C and 1 h under a pressurized atmosphere of H_2 (5 MPa).

Scheme 2. (**A**) Hydrodesulfurization (HDS) of dibenzothiophene (DBT) via the desulfurization (DDS) and hydrogenation (HYD) pathways, (**B**) HDS of 4,6-dimethyldibenzothiophene (DMDBT) via the DDS and HYD pathways, (**C**) hydrodeoxygenation (HDO) of stearic acid through the DeCO$_x$ and HYD pathways, (**D**) hydrodenitrogenation (HDN) of quinoline through the denitrogenation (DDN) and HYD pathways, and (**E**) HYD of tetralin to *cis*- and *trans*-decalin.

The selectivity of mesoporous sulfide catalysts in these model reactions is also influenced by the competitive adsorption of various model compounds on the catalytically active sites (Figure 7). For the mesoporous CoMo/γ-Al$_2$O$_3$ sulfide catalyst, the selectivity for the DDS of DBT was decreased by stearic acid, increased by quinoline, and remained nearly unchanged if both model compounds are present. The reverse is true for the selectivity for the HYD of tetralin to *cis*-decalin. On the other hand, the selectivity for the DDS of DMDBT was increased by stearic acid and, in particular, quinoline. The selectivity for the DDN of quinoline and the DeCOx of stearic acid was subject to slight variation. For the mesoporous NiMo/γ-Al$_2$O$_3$ sulfide catalyst, the selectivity for the DDS of DBT and DMDBT was positively influenced by stearic acid and, in particular, quinoline, while the selectivity for the DeCO$_x$ of stearic acid was decreased by quinoline. The latter observation is similar to those of a recent study reported by Deliy et al. [27]. They showed that the DeCO$_x$ products were mainly formed during the HDO of methyl palmate over sulfided NiMo/γ-Al$_2$O$_3$ catalyst, preferably in the presence of aromatic molecules. The selectivity for the HYD of tetralin to *cis*-decalin and the DDN of quinoline is subject to slight variation. With these results in mind, we can presume that the nitrogen atom in quinoline has a greater influence on the selectivity of mesoporous sulfide catalysts in the hydrotreating of model diesel oils than other heteroatoms present in the model compounds. In addition, these model compounds influence the reaction pathways over mesoporous CoMo/γ-Al$_2$O$_3$ and NiMo/γ-Al$_2$O$_3$ sulfide catalysts differently, presumably associated with the differences in binding strength and spatial location of reactant molecules on the catalytically active sites.
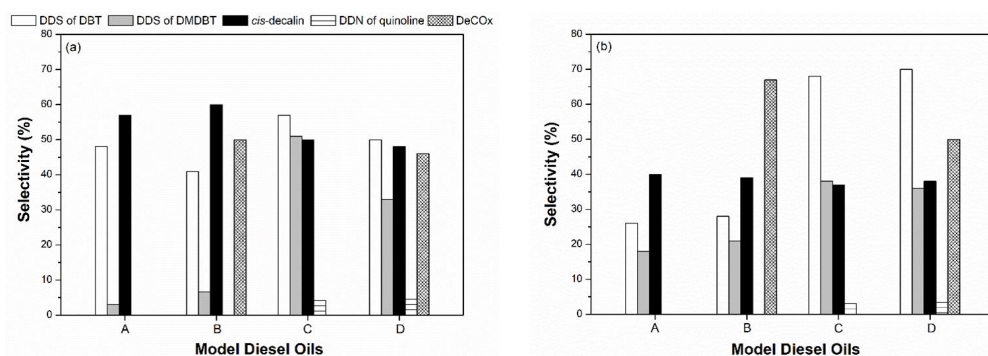
Figure 7. The selectivity of the mesoporous sulfide catalysts (**a**) CoMo/γ-Al$_2$O$_3$ and (**b**) NiMo/γ-Al$_2$O$_3$ in the hydrotreating of model diesel oils A–D at 330 °C and 5 MPa of H$_2$ for 1 h.

Recent studies have shown that the catalytic activity and selectivity of mesoporous CoMo/γ-Al$_2$O$_3$ and NiMo/γ-Al$_2$O$_3$ sulfide catalysts in the hydrotreating of petroleum- and coal-derived oils are not only associated with surface fine structures of Co- and Ni-incorporated MoS$_2$-like slabs as the catalytically active sites, but also strongly influenced by the spatial location of heteroatom-containing compounds, such as H$_2$S or amines, competitively adsorbed on the catalytically active sites [25,26,28–33]. In the HDS of DBT and DMDBT, it is generally agreed that the catalytically active sites for the DDS pathway are associated with the CUS regions at the edges or corners of Co- and Ni-incorporated MoS$_2$-like slabs, so-called the Co(Ni)-Mo-S structures, while those for the HYD pathway are related to the brim sites, which exhibit metal-like character [25,26]. In the upgrading of model diesel oil A over the mesoporous CoMo/γ-Al$_2$O$_3$ sulfide catalyst, there is no doubt that small Co-incorporated MoS$_2$-like slabs with high stacking numbers are highly efficient in the HDS of DBT toward the DDS product, which is catalyzed by the Co-Mo-S structures at the edges or corners. In contrast, the main HDS route of DMDBT is the HYD pathway, which is catalyzed by the brim sites because of steric hindrance [31]. The hydrotreating activity of the mesoporous NiMo/γ-Al$_2$O$_3$ sulfide catalyst in the hydrotreating of model diesel oil A is poor by comparison, suggesting that large Ni-incorporated MoS$_2$-like slabs with lower stacking numbers contain relatively low numbers of catalytically active sites, i.e., the Ni-Mo-S structures, and show relatively low activity for HDS reactions. However, the HYD of tetralin to *trans*-decalin over the brim sites is significantly enhanced, presumably because of the high electron density of the brim sites, which facilitate hydrogen dissociation corresponding to the high HYD ability of the large Ni-incorporated MoS$_2$-like slabs [25]. The variation in selectivity for the HDS of DBT and DMDBT over the mesoporous sulfide catalysts could be related to their competitive adsorption on the catalytically active sites.

In the hydrotreating of model diesel oils B–D, the hydrotreating activity and selectivity of mesoporous sulfide catalysts in the HDS of DBT and DMDBT and the HYD of tetralin varied intensely. In the case of the mesoporous CoMo/γ-Al$_2$O$_3$ sulfide catalyst, we speculate that a considerable number of the Co-Mo-S structures are occupied or hindered by the adsorption of stearic acid and, in particular, quinoline. The DDS pathway in the HDS of DBT was slightly inhibited, whereas the reverse is true for the DDS pathway in HDS of DMDBT. The selectivity of *cis*-decalin was slightly enhanced by stearic acid although the HYD of tetralin was inhibited. Clearly, stearic acid occupies the Co-Mo-S structures and is quickly converted to the hydrotreated products (*n*-heptadecane and *n*-octadecane) under the severe reaction conditions. As a result, the HDS of DBT to the DDS product was negatively affected by the presence of stearic acid and its hydrotreated products. The HDS of DMDBT was slightly enhanced, presumably because more DMDBT is accessible to the catalytically active sites. This might be because the solvent environment near the catalytically active sites, such as the hydrophobic–hydrophilic properties, was affected by the hydrotreated products derived from the HDO of stearic acid. By comparison, quinoline promoted the HDS of DMDBT toward the DDS product remarkably, although the conversion was extremely low. In addition, the influence of quinoline on the

HDS of DBT toward the DDS product was positive with a slight decrease in conversion. The results cannot be simply explained in the same way. According to recent studies reported by Prins et al., Lauritsen et al., and other pioneers, the DDS pathway occurs by the σ-adsorption of DMDBT on the Co-Mo-S structures via the sulfur atom, while the HYD pathway presumably proceeds by π-adsorption of DMDBT on the brim sites via the aromatic system [25–32]. In this study, presumably, the quinoline molecules can be adsorbed either on the Co-Mo-S structures or the brim sites of the Co-incorporated MoS_2-like slabs [33]. The π-adsorption of bulky DMDBT molecules with two methyl groups in the 4 and 6 positions on the residual sites of the Co-incorporated MoS_2-like slabs is the first step of the HYD pathway and is significantly inhibited by steric hindrance (Scheme S1). This means that more DMDBT is available for the DDS pathway through the σ-adsorption of DMDBT via the sulfur atoms because this results in less steric hindrance. In the case of the mesoporous $NiMo/\gamma\text{-}Al_2O_3$ sulfide catalyst, the HDS of DBT and DMDBT was not negatively influenced by quinoline, and the selectivity toward the DDS product was also facilitated. Moreover, the influence of stearic acid on selectivity for the HDS of DBT and the HYD of tetralin was nearly negligible. This might be associated with the special surface properties of the mesoporous $NiMo/\gamma\text{-}Al_2O_3$ sulfide catalyst; that is, (i) the number of the Ni-Mo-S structures for the DDS pathway is originally low, (ii) the brim sites with enhanced metallic properties have high HYD activity, and (iii) the adsorption strengths of stearic acid and quinoline on surface sites with relatively low CUS and weak acidity are supposedly low. Similarly, the desorption of the HDO and HDN products should be facilitated. Because of these special surface properties, the poisoning of the mesoporous $NiMo/\gamma\text{-}Al_2O_3$ sulfide catalyst by stearic acid and quinoline becomes less intense.

2.3. Co-Processing of Jatropha Bio-Oil with Model Diesel Oil or LGO

The catalytic performance of sulfided catalysts in the co-processing of Jatropha bio-oil mixed with model diesel oil A' or LGO, denoted as oil feedstocks E and F, respectively, was further examined using a stainless-steel batch-type reactor at 330–350 °C and 5–7 MPa of H_2 for 3 h. The catalyst weight was varied in range of 10–20 wt % based on the oil feedstocks. The oil feedstocks made by mixing model diesel oil A' (or LGO) with 10 wt % Jatropha bio-oil have high acid values in the range of 5.8–7.3 mg KOH g^{-1}. Jatropha bio-oil mainly consists of fatty acids and derivatives, in addition to small amounts of hydrocarbons and oxygen- and nitrogen-containing aromatic compounds, based on the gas chromatography–flame ionization detector (GC-FID) and gas chromatography–mass spectrometry (GC-MS) analyses (Figures S1–S2, ESI). In Table 2, the results show again that the mesoporous $NiMo/\gamma\text{-}Al_2O_3$ sulfide catalyst is superior to the mesoporous $CoMo/\gamma\text{-}Al_2O_3$ sulfide catalyst in the simultaneous removals of sulfur, nitrogen, and oxygen from Jatropha bio-oil co-fed with model diesel oil A' or LGO. The hydrotreating activity of mesoporous sulfide catalysts was decreased by replacing model diesel oil A' with LGO. It appears likely that the aromatic sulfur compounds present in LGO are complex, making sulfur removal a difficult task. On the other hand, in addition to decreasing the hydrogen partial pressure during the reaction period, the byproducts formed during the HDS, HDO, and HDN processes, such as H_2S, H_2O, and NH_3, may occupy the catalytically active sites of mesoporous sulfide catalysts in a batch-type reactor (a closed system), and presumably cause catalyst deactivation. Hydrotreated oils with moderate sulfur contents (46–116 ppm) were only obtained under severe reaction conditions. To overcome these technical problems, the co-processing of Jatropha bio-oil with LGO over the mesoporous $NiMo/\gamma\text{-}Al_2O_3$ sulfide catalyst was further performed in an up-flow fixed-bed reactor at 350 °C and 5–7 MPa of H_2 flow (150 Ncc min^{-1}) using a weight hourly space velocity (WHSV) value of 1.5 h^{-1}. After a time-on-stream (TOS) period of 96 h, the hydrotreated oils with low sulfur contents and almost no oxygen and nitrogen were obtained, particularly when the hydrogen pressure was increased to 7 MPa. The GC profiles show that the hydrotreated oil derived from the co-processing of Jatropha bio-oil with LGO over the mesoporous $NiMo/\gamma\text{-}Al_2O_3$ sulfide catalyst at 350 °C and 7 MPa of H_2 flow is similar to petrodiesel fuel (Figure 8). In other words, the hydrotreated oil with reduced carbon footprint is a potential source of drop-in diesel-like fuel and is expected to be a greener fuel for the transport sector with low environmental impact.

Table 2. Upgrading of Jatropha bio-oil co-fed with the model diesel oil or light gas oil (LGO) over the mesoporous sulfide catalysts.

Sulfided Catalysts	Reaction Condition						Hydrotreating Activity $(mmol\ g \cdot cat^{-1}\ h^{-1})$	Hydrotreated Oils		
	Reactor	Feedstock [a]	T (°C)	P_{H2} (MPa)	Period (h)	W_{Catal} (wt %)		S (ppm)	N (ppm)	Acid Value $(mg\ KOH\ g^{-1})$
CoMo/γ-Al$_2$O$_3$	Batch-type	E	330	5	3	10	0.44	470	57	0.068
		F	330	5	3	10	0.37	790	0	0.060
NiMo/γ-Al$_2$O$_3$	Batch-type	E	330	5	3	10	0.50	260	0	0.079
		F	330	5	3	10	0.40	560	0	0.077
		F	330	7	3	10	0.50	264	0	0.079
		F	330	7	3	20	0.52	116	0	0.068
		F	350	7	3	10	0.65	46	0	0.061
	Fixed-bed	F	350	5	WHSV = 1.5 h^{-1}		0.12	60	15	0.033
		F	350	7	WHSV = 1.5 h^{-1}		0.13	12	6.0	0.034

[a] Oil feedstock E is a mixture of Jatropha bio-oil (ca. 10 wt %) and model diesel oil A', which consisted of hexadecane (70 wt %), tetralin (30 wt %), and sulfur-containing compounds (2500 ppm; 95% DBT and 5% DMDBT), and the sulfur content, nitrogen content, and acid value of oil feedstock E are 2425 ppm, 2600 ppm, and 7.3 mg KOH g^{-1}, respectively. Oil feedstock F is a mixture of Jatropha bio-oil (ca. 10 wt %), and LGO, and its sulfur content, nitrogen content, and acid value are 2724 ppm, 2450 ppm, and 5.84 mg KOH g^{-1}, respectively.
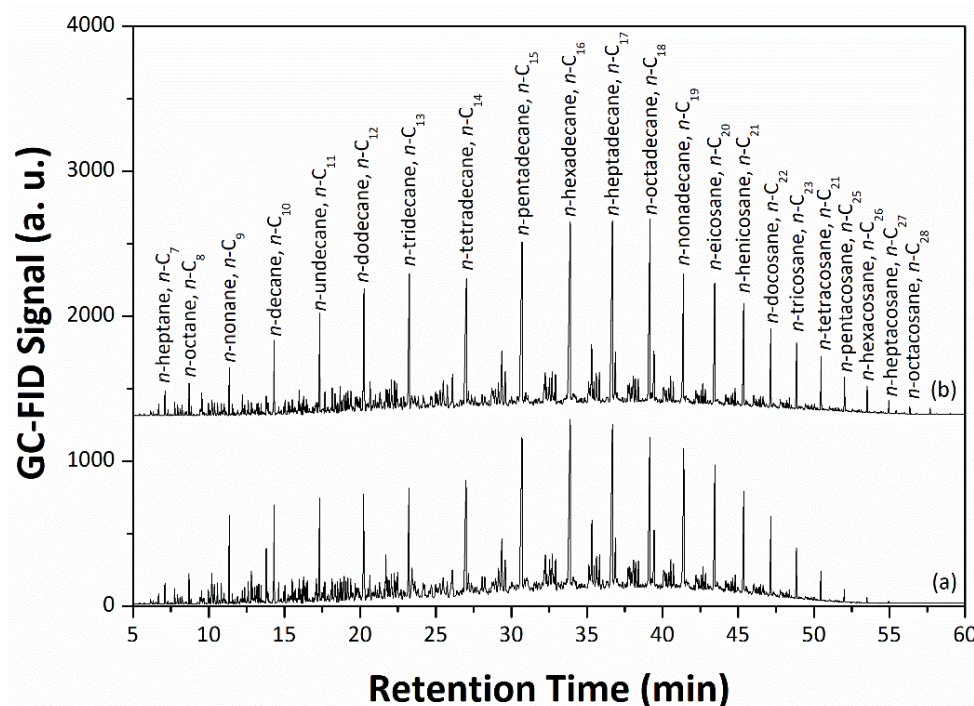
Figure 8. Gas chromatography–mass spectrometry (GC-FID) profiles of (a) commercially available petroleum diesel and (b) hydrotreated oil, which was produced by hydrotreating Jatropha bio-oil (10 wt %) co-fed with LGO over the mesoporous NiMo/γ-Al$_2$O$_3$ sulfide catalyst on an up-flow fixed-bed reaction system (350 °C, 7 MPa of H$_2$ and 1.5 h^{-1} of WHSV).

3. Material and Methods

3.1. Synthesis of Mesoporous Sulfide Catalysts

A modified recipe for the preparation of mesoporous sulfide catalysts, which would be suitable for upgrading Jatropha bio-oil co-fed with petroleum distillates, was developed from our previous studies on hydrotreating catalysts for the conventional diesel HDS process [17–19]. A commercial support of γ-Al$_2$O$_3$ was kindly provided by a Japanese catalyst company. The BET specific area, porosity and acid capacity of γ-Al$_2$O$_3$ are 219 m^2 g^{-1}, 0.759 cm^2 g^{-1} and 0.70 mmol g^{-1}, respectively. Typically, the mesoporous CoMo/γ-Al$_2$O$_3$ and NiMo/γ-Al$_2$O$_3$ sulfide catalysts were prepared by an incipient wetness impregnation method using citric acid-stabilized CoMo and NiMo precursor solutions, denoted CoMo(cit) and NiMo(cit), respectively. The molar compositions of homemade CoMo(cit) and NiMo(cit) precursor solutions were MoO$_3$:(CoO or NiO):C$_6$H$_8$O$_7$:H$_2$O = 1.0:0.5:0.58:1.67. The impregnated samples containing 23.6 wt % of MoO$_3$ and 6.1 wt % of CoO (or NiO) were dried under microwave irradiation (1050 W, 50 Hz) for 10 min, followed by sulfidation at 360 °C for 3 h under a 5%H$_2$S/H$_2$ flow (50 mL min^{-1}). As a result, the mesoporous CoMo/γ-Al$_2$O$_3$ and NiMo/γ-Al$_2$O$_3$ sulfide catalysts were prepared.

3.2. Characterization

The wide-angle XRD patterns were recorded using a Bruker AXS D8 advance diffractometer using a Cu Kα radiation (λ = 1.5418 Å). The nitrogen adsorption-desorption isotherms were measured by a BELSORP-28A instrument at 77 K. Before the measurements, the mesoporous sulfide catalysts were outgassed at 120 °C for 200 min under high vacuum (<20 Pa). The differential heat of ammonia adsorption over the mesoporous sulfide catalysts was measured by a CSA-450G instrument equipped with a micro-calorimeter (Tokyo Riko, Co., Ltd., Tokyo) at 50 °C. Before the experiments, the mesoporous sulfide catalysts were obtained by the sulfidation (the same procedures as shown in

Section 3.1), and then degassed under vacuum (~10^{-4} torr). The uptake of nitric oxide over the mesoporous sulfide catalysts was determined by an Ohkura Riken R6015 instrument at 50 °C. Before the experiments, the mesoporous sulfide catalysts were obtained by the sulfidation (the same procedures as shown in Section 3.1), followed by purging with helium flow (50 mL min^{-1}) until the TCD signal was stable. The DRIFT spectra of mesoporous sulfide catalysts adsorbed with pyridine and NO were recorded on a Thermo Nicolet Nexus 870 FI-IR instrument equipped with an in situ DRIFT cell at 100 °C. Before the measurements, the passivated samples were sulfided again at 360 °C for 3 h under a 5%H_2S/H_2 flow (50 mL min^{-1}). High-resolution transmission electron microscope (HRTEM) experiments were performed on a TOPCON EM002B instrument operating with a 120-keV electron gun.

3.3. Co-Processing of Jatropha Bio-Oil and Petroleum Distillates

The catalytic performance of mesoporous sulfide catalysts in the upgrading of model diesel oils A–D was examined using a high-pressure stainless-steel reactor (480 mm in length and 9 mm in internal diameter, 30.5 mL) at 330 °C and 5 MPa of H_2 for 1 h. For the model reactions, the weights of model diesel oils and mesoporous sulfide catalysts were kept at 8.0 and 0.8 g, respectively. The model diesel oil was made up of 70 wt % n-hexadecane ($C_{16}H_{34}$, Sigma-Aldrich, St. Louis, MI, USA) and 30 wt % tetralin ($C_{10}H_{12}$, Wako, Tokyo, Japan). The model diesel oils A-D were then cautiously prepared by mixing the model diesel oil with proper amounts of model compounds (Table S1, ESI, New Delhi, India). Dibenzothiophene (DBT, $C_{12}H_8S$, Sigma-Aldrich) and 4,6-dimethyldibenzothiophene (DMDBT, $C_{14}H_{12}S$, Sigma-Aldrich) were used as sulfur-containing model compounds of crude diesel oil, whereas stearic acid ($C_{18}H_{36}O_2$, Wako) and quinoline (C_9H_7N, Wako) were used as oxygen- and nitrogen-containing model compounds of Jatropha bio-oil, respectively. Note that small amounts of quinoline were present in the crude diesel oil. The model diesel oil A was prepared to mimic LGO while the model diesel oils B-C were prepared to mimic the low-grade oil feedstocks for the co-processing of Jatropha bio-oil with LGO. Typically, model diesel oil A was prepared by mixing of model diesel oil with 3500 ppm of sulfur-containing compounds (50 wt % of BDT and 50 wt % of DMDBT). To analyze the compositions of the hydrotreated products easily, a relatively large amount of DMDBT was used. Model diesel oil B with an additional 1.5 wt % of oxygen was prepared by adding stearic acid to model diesel oil A. The model diesel oil C with additional 3500 ppm of nitrogen was prepared by adding quinoline to model diesel oil A. Model diesel oil D with an additional 1.5 wt % of oxygen and 3500 ppm of nitrogen was prepared by adding stearic acid and quinoline, respectively, to the model diesel oil A.

The co-processing of low-grade feedstock oils (denoted as E and F) over the mesoporous sulfide catalysts was further studied using a batch-type stainless steel reactor at 330–350 °C and 5–7 MPa of H_2 for 3 h. The feedstocks E and F were prepared by dissolving Jatropha bio-oil (10 wt %) in model diesel oil A' and LGO, respectively. Model diesel oil A' was prepared by the mixing of model diesel oil with 2500 ppm of sulfur-containing compounds (95% of DBT and 5% of DMDBT). The amounts of mesoporous sulfide catalysts were varied at 10–20 wt % of the oil feedstocks E and F. In some cases, the co-processing of Jatropha bio-oil with LGO over the mesoporous sulfide catalysts was performed on a continuous up-flow fixed-bed reaction system at 350 °C and 5–7 MPa of H_2 (150 Ncc min^{-1}). The WHSV of oil feedstock F was kept at 1.5 h^{-1}. For a TOS of 96 h, the hydrotreated oils were qualitatively and quantitatively analyzed by Agilent 5795 GC/MS (Agilent Technologies Inc, Santa Clara, CA, USA) and 6890N CG/FID instruments (Agilent Technologies Inc, Santa Clara, CA, USA) equipped with HP-1 columns (60 m in length, 0.25 mm in diameter, 0.25 μm in film thickness), respectively. The sulfur and nitrogen contents were measured by a Mitsubishi TS-100V trace sulfur and nitrogen analyzer (Mtsubishi Chemical Corporation, Kanagawa, Japan). The acid value was measured by a Metrohm 809 Titrando autotitrator (Metrohm AG, Herisau, Switzerland).

4. Conclusions

The catalytic performance of mesoporous sulfide catalysts ($CoMo/\gamma$-Al_2O_3 and $NiMo/\gamma$-Al_2O_3) in the co-processing of an unconventional type of Jatropha bio-oil with petroleum distillates had been thoroughly studied by model reactions and the industrial diesel HDS process using a batch-type reactor and fixed-bed reaction system under severe reaction conditions. The mesoporous $CoMo/\gamma$-Al_2O_3 sulfide catalyst was highly active for the conventional HDS reaction, but it was deactivated in the co-processing of the oil feedstocks containing oxygen- and nitrogen-containing compounds, which formed tightly adsorbed fouling species on the catalytically active sites. In contrast, the mesoporous $NiMo/\gamma$-Al_2O_3 sulfide catalyst with high HYD ability and low affinity to sulfur-, oxygen- and nitrogen-containing compounds was highly active in the simultaneous removal of those heteroatoms from the oil feedstocks during the upgrading process. As a result, the hydrotreated oil with nearly no heteroatoms is a potential source of drop-in diesel-like fuel for use as a greener fuel that can reduce the impact of the transport sector on the environment. It is also expected that low-grade oil feedstocks or next-generation bio-oils derived from algae and non-edible biomass with large amounts of oxygen- and nitrogen-containing compounds could be catalytically transformed into high-quality transport fuels under the hydrotreating conditions reported in this work.

Author Contributions: S.-Y. Chen conceived, designed and performed the experiments; M. Nishi analyzed the data and assisted in manuscript editing; A. Takatsuki and W. Roschat performed the experiments; T. Mochizuki, H. Takagi, M. Toba, and Y. Yoshimura provided suggestions; S.Y. Chen wrote the paper.

References

1. International Energy Agency. World Energy Outlook Special Report 2015: Energy and Climate Change. Available online: https://www.iea.org/publications/freepublications/publication/WEO2015SpecialReportonEnergyandClimateChange.pdf (accessed on 15 June 2015).

2. Energy and Environment Partnership/Mekong. The Alternative Energy Development Plan 2015–2036 (AEPD2015-2036). Available online: http://eepmekong.org/index.php/resources/country-reports/thailand/191-alternative-energy-development-plan-2015--2036-in-thai/file (accessed on 18 September 2015).

3. Amorin, H.V.; Lopes, M.L.; Oliveira, J.V.C.; Buckeridge, M.S.; Goldman, G.H. Scientific challenges of bioethanol production in Brazil. *Appl. Microbiol. Biotechnol.* **2011**, *91*, 1267–1275. [CrossRef] [PubMed]

4. Lee, A.F.; Bennett, J.A.; Manayil, J.C.; Wilson, K. Heterogeneous catalysis for sustainable biodiesel production via esterification and transesterification. *Chem. Soc. Rev.* **2014**, *43*, 7887–7916. [CrossRef] [PubMed]

5. Nizami, A.S.; Korres, N.E.; Murphy, J.D. Review of the integrated process for the production of grass biomethane. *Environ. Sci. Technol.* **2009**, *43*, 8496–8508. [CrossRef] [PubMed]

6. Huber, G.W.; Iborra, S.; Corma, A. Synthesis of transportation fuels from biomass: Chemistry, catalysts, and engineering. *Chem. Rev.* **2006**, *106*, 4044–4098. [CrossRef] [PubMed]

7. Serrano-Ruiz, J.C.; Dumesic, J.A. Catalytic routes for the conversion of biomass into liquid hydrocarbon transportation fuels. *Energy Environ. Sci.* **2011**, *4*, 83–99. [CrossRef]

8. Liu, C.; Wang, H.; Karim, A.M.; Sun, J.; Wang, Y. Catalytic fast pyrolysis of lignocellulosic biomass. *Chem. Soc. Rev.* **2014**, *43*, 7594–7623. [CrossRef] [PubMed]

9.   Mochizuki, T.; Atong, D.; Chen, S.Y.; Toba, M.; Yoshimura, Y. Effect of SiO$_2$ pore size on catalytic fast pyrolysis of Jatropha residues by using pyrolyzer-GC/MS. *Catal. Commun.* **2013**, *36*, 1–4. [CrossRef]

10.   Mochizuki, T.; Chen, S.Y.; Toba, M.; Yoshimura, Y. Deoxygenation of guaiacol and woody tar over reduced catalysts. *Appl. Catal. B Environ.* **2014**, *146*, 237–243. [CrossRef]

11.   Grilc, M.; Likozar, B.; Levec, J. Hydrodeoxygenation and hydrocracking of solvolysed lignocellulosic biomass by oxide, reduced and sulphide form of NiMo, Ni, Mo and Pd catalysts. *Appl. Catal. B Environ.* **2014**, *150–151*, 275–287. [CrossRef]

12.   Kubička, D.; Horáček, J. Deactivation of HDS catalysts in deoxygenation of vegetable oils. *Appl. Catal. A Gen.* **2011**, *394*, 9–17. [CrossRef]

13.   Toba, M.; Abe, Y.; Kuramochi, H.; Osako, M.; Mochizuki, T.; Yoshimura, Y. Hydrodeoxygenation of waste vegetable oil over sulfide catalysts. *Catal. Today* **2011**, *164*, 533–537. [CrossRef]

14.   Mochizuki, T.; Toba, M.; Yoshimura, Y. Fast pyrolysis of Jatropha residues over zeolite catalysts. *J. Jpn. Petrol. Inst.* **2012**, *55*, 69–70. [CrossRef]

15.   Mochizuki, T.; Toba, M.; Yoshimura, Y. Effect of electrostatic precipitator on collection efficiency of bio-oil in fast pyrolysis of biomass. *J. Jpn. Petrol. Inst.* **2013**, *56*, 401–405. [CrossRef]

16.   Mochizuki, T.; Chen, S.Y.; Toba, M.; Yoshimura, Y. Pyrolyzer–GC/MS system-based analysis of the effects of zeolite catalysts on the fast pyrolysis of Jatropha husk. *Appl. Catal. A Gen.* **2013**, *456*, 174–181. [CrossRef]

17.   Hiroshima, K.; Mochizuki, T.; Honma, T.; Shimizu, T.; Yamada, M. High HDS activity of Co-MoAl$_2$O$_3$ modified by some chelates and their surface fine structures. *Appl. Surf. Sci.* **1997**, *121–122*, 433–436. [CrossRef]

18.   Parry, E.P. An infrared study of pyridine adsorbed on acidic solids. Characterization of surface acidity. *J. Catal.* **1963**, *2*, 371–379. [CrossRef]

19.   Chen, S.Y.; Lao-ubol, S.; Mochizuki, T.; Abe, Y.; Toba, M.; Yoshimura, Y. Transformation of non-edible vegetable oils into biodiesel fuels catalyzed by unconventional sulfonic acid-functionalized SBA-15. *Appl. Catal. A Gen.* **2014**, *485*, 28–39. [CrossRef]

20.   Chen, S.Y.; Mochizuki, T.; Abe, Y.; Toba, M.; Yoshimura, Y.; Somwongsa, P.; Lau-ubol, S. Carbonaceous Ti-incorporated SBA-15 with enhanced activity and durability for high-quality biodiesel production: Synthesis and utilization of the P123 template as carbon source. *Appl. Catal. B Environ.* **2016**, *181*, 800–809. [CrossRef]

21.   Shimizu, T.; Hiroshima, K.; Honma, T.; Mochizuki, T.; Yamada, M. Highly active hydrotreatment catalysts prepared with chelating agents. *Catal. Today* **1998**, *45*, 271–276. [CrossRef]

22.   Yoshimura, Y.; Matsubayashi, N.; Sato, T.; Shimada, H.; Nishijima, A. Molybdate catalysts prepared by a novel impregnation method: Effect of citric acid as a ligand on the catalytic activities. *Appl. Catal. A Gen.* **1991**, *79*, 145–159. [CrossRef]

23.   Yoshimura, Y.; Toba, M.; Matsubayashi, N.; Matsui, T. Hydrotreating Catalyst of Catalytic Cracking Gasoline. U.S. Patent US20050261124 A1, 24 November 2005.

24.   Yoshimura, Y.; Toba, M.; Matsubayashi, N.; Matsui, T. Hydrotreating Catalyst of Catalytic Cracking Gasoline. U.S. Patent US7393807 B2, 1 July 2008.

25.   Hrabar, A.; Hein, J.; Gutiérrez, O.Y.; Lercher, J.A. Selective poisoning of the direct denitrogenation route in o-propylaniline HDN by DBT on Mo and NiMo/γ-Al$_2$O$_3$ sulfide catalysts. *J. Catal.* **2011**, *281*, 325–338. [CrossRef]

26.   Prins, R.; Egorova, M.; Röthlisberger, A.; Zhao, Y.; Sivasankar, N.; Kukula, P. Mechanisms of hydrodesulfurization and hydrodenitrogenation. *Catal. Today* **2006**, *111*, 84–93. [CrossRef]

27.   Deliy, I.V.; Vlasova, E.N.; Nuzhdin, A.L.; Gerasimov, E.Y.; Bukhtiyarova, G.A. Hydrodeoxygenation of methyl palmitate over sulfided Mo/Al$_2$O$_3$, CoMo/Al$_2$O$_3$ and NiMo/Al$_2$O$_3$ catalysts. *RSC Adv.* **2014**, *4*, 2242–2250. [CrossRef]

28.   Toba, M.; Miki, Y.; Kanda, Y.; Matsui, T.; Harada, M.; Yoshimura, Y. Selective hydrodesulfurization of FCC gasoline over CoMo/Al$_2$O$_3$ sulfide catalyst. *Catal. Today* **2005**, *104*, 64–69. [CrossRef]

29.   Yoshimura, Y.; Sato, T.; Shimada, H.; Matsubayashi, N.; Nishijima, A. Influences of oxygen-containing substances on deactivation of sulfided molybdate catalysts. *Appl. Catal.* **1991**, *73*, 55–63. [CrossRef]

30.   Prins, R.; Zhao, Y.; Sivasankar, N.; Kukula, P. Mechanism of CN bond breaking in hydrodenitrogenation. *J. Catal.* **2005**, *234*, 509–512. [CrossRef]

31. Egorova, M.; Prins, R. The role of Ni and Co promoters in the simultaneous HDS of dibenzothiophene and HDN of amines over Mo/γ-Al$_2$O$_3$ catalysts. *J. Catal.* **2006**, *241*, 162–172. [CrossRef]

32. Lauritsen, J.V.; Nyberg, M.; Nørskov, J.K.; Clausen, B.S.; Topsøe, H.; Lægsgaard, E.; Besenbacher, F. Hydrodesulfurization reaction pathways on MoS$_2$ nanoclusters revealed by scanning tunneling microscopy. *J. Catal.* **2004**, *224*, 94–106. [CrossRef]

33. Rangarajan, S.; Mavrikakis, M. DFT insights into the competitive adsorption of sulfur- and nitrogen-containing compounds and hydrocarbons on Co-promoted molybdenum sulfide catalysts. *ACS Catal.* **2016**, *6*, 2904–2917. [CrossRef]